RESEARCH REPORTS
Biomaterials & Bioengineering

R.K. Nalla[1], J.H. Kinney[2], S.J. Marshall[2], and R.O. Ritchie[1]*

[1]Materials Sciences Division, Lawrence Berkeley National Laboratory, and Department of Materials Science and Engineering, Hearst Mining Building, University of California, Berkeley, CA 94720; and [2]Department of Preventive and Restorative Dental Sciences, University of California, San Francisco, CA 94143; *corresponding author, RORitchie@lbl.gov

J Dent Res 83(3):211-215, 2004

On the *in vitro* Fatigue Behavior of Human Dentin: Effect of Mean Stress

ABSTRACT

Human dentin is susceptible to failure under repetitive cyclic-fatigue loading. This investigation seeks to address the paucity of data that reliably quantify this phenomenon. Specifically, the effect of alternating *vs.* mean stresses, characterized by the stress- or load-ratio *R* (ratio of minimum-to-maximum stress), was investigated for three *R* values (-1, 0.1, and 0.5). Dentin was observed to be prone to fatigue failure under cyclic stresses, with susceptibility varying, depending upon the stress level. The "stress-life" (*S/N*) data obtained are discussed in the context of constant-life diagrams for fatigue failure. The results provide the first fatigue data for human dentin under tension-compression loading and serve to map out safe and unsafe regimes for failure over a wide range of *in vitro* fatigue lives ($< 10^3$ to $> 10^6$ cycles).

KEY WORDS: dentin, fatigue, *S/N* behavior, stress-ratio, fractography, constant-life diagram.

INTRODUCTION

Dentin, the most abundant mineralized tissue in teeth, is a hydrated composite of collagen fibrils and nanocrystalline apatite (Kinney *et al.*, 2003). Fluid-filled cylindrical tubules course from the dentin-enamel and cementum-enamel junctions to the pulp; they are surrounded by a thin, highly mineralized peritubular dentin cuff. The mineralized collagen fibrils are arranged orthogonally to the tubules (Jones and Boyde, 1984), forming a planar, felt-like structure called the intertubular dentin matrix. Since dentin forms the bulk of the human tooth and is critical to its structural integrity, an understanding of its mechanical properties is important for life prediction, particularly because of the effect of microstructural modifications from caries, sclerosis, aging, and restorative processes. While several studies have focused on evaluating the properties of dentin (*e.g.*, Craig and Peyton, 1958; Lehman, 1967; Rasmussen *et al.*, 1976; Goodis *et al.*, 1993; Sano *et al.*, 1994; Tonami and Takahashi, 1997; Arola *et al.*, 2002; Kinney *et al.*, 2003; Nalla *et al.*, 2003a), there are only limited data on the role of fatigue loading in affecting the mechanical behavior of dentin (Tonami and Takahashi, 1997; Arola *et al.*, 2002; Nalla *et al.*, 2003a).

Exposed root surfaces commonly exhibit non-caries lesions in the form of notches in the dentin just below the enamel-cementum junction. The etiology for such lesions is believed to involve a combination of erosion, abrasion, and abfraction (Levitch *et al.*, 1994). Such notches serve as effective stress-raisers and sites of fracture-induced failure. While cusp fractures sometimes occur in posterior teeth, anterior teeth are more susceptible to fracture at the gingiva, severing the crown. Although such fractures have not been studied extensively, it is believed that tooth failure is often associated with either catastrophic events induced by high occlusal stresses or subcritical crack-growth induced by cyclic (fatigue) loading (Wiskott *et al.*, 1995).

To date, only limited studies have been performed on fatigue in dentin. Tonami and Takahashi (1997) used a "staircase" method to determine values of 46.9-51.0 MPa for the 10^5-cycle endurance strength of bovine dentin, the lower value being obtained for dentin from older animals. Although this study suggested an effect of aging, it was restricted to a narrow range of purely tensile stress-ratios (R = 0.15-0.25), a low number of cycles to failure (10^5-cycle fatigue strengths may not be "conservative", since a typical human tooth experiences ~ 10^6 cycles annually), and tests in water rather than simulated body fluid, raising concerns of demineralization. [The stress (or load) ratio, *R*, defined as the ratio of the minimum-to-maximum stress (or load), is a measure of the magnitude of the mean *vs.* alternating stresses (or loads); see Fig. 1a.] More recently, Arola *et al.* (2002) reported preliminary results on fatigue-crack growth rates for various orientations in bovine dentin. Using zero-to-tension cycling at 2- to 5-Hz frequency in saline, they reported that propagation rates were highest perpendicular to the tubules. Nalla *et al.* (2003a)

Received March 27, 2003; Last revision July 28, 2003; Accepted December 15, 2003

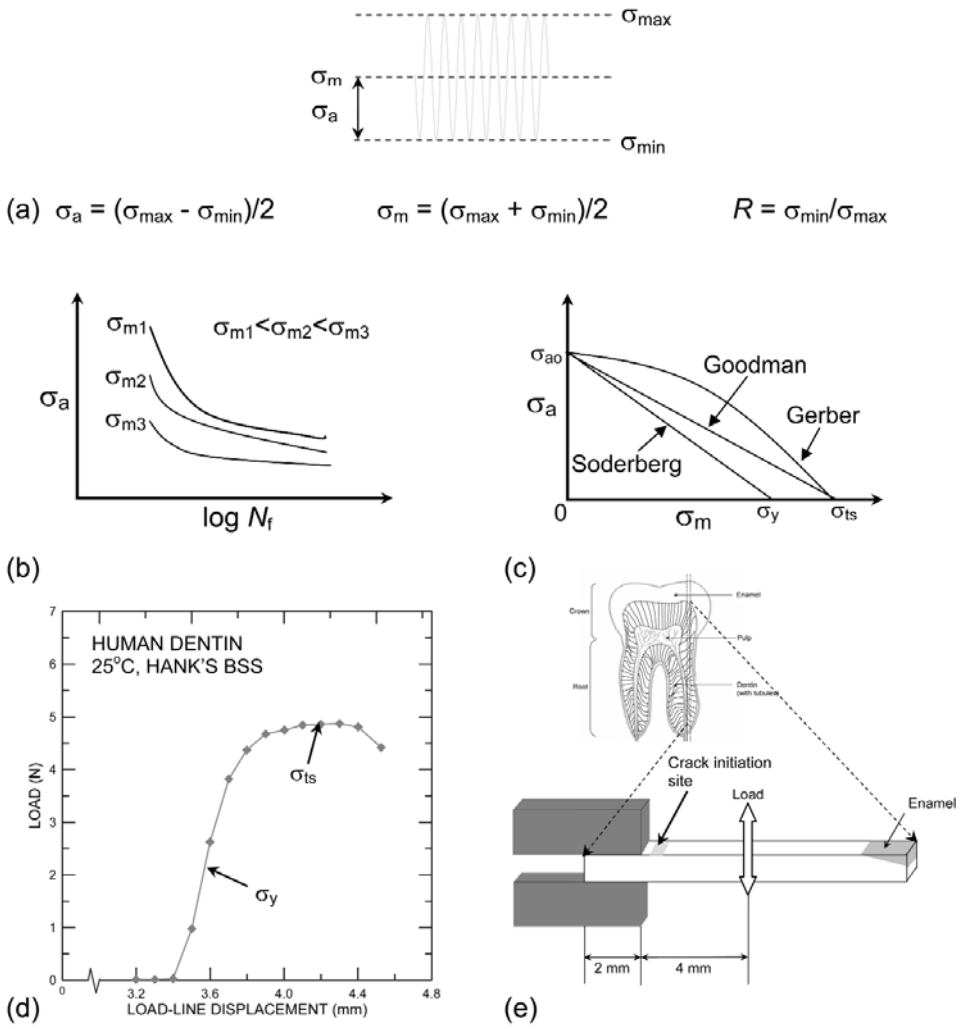

Figure 1. Fatigue theory and experimental set-up. Schematic illustrations of **(a)** the definition of the various stresses associated with a fatigue cycle, **(b)** typical stress-amplitude (σ_a)-life (N_f) (*S/N*) plots for different mean-stress (σ_m) levels, and **(c)** constant life (σ_a-σ_m) curves. **(d)** Load-displacement curve obtained in bending, showing loads used to obtain σ_y (at deviation from linearity of elastic part of the curve) and σ_{ts} (at maximum load). (e) Schematic of cantilever-beam geometry used for fatigue stress-life testing. Each dentin beam, which is mechanically clamped at one end, included some root dentin and coronal dentin. Inset shows sections cut from the molar in relation to the tubule curvature. For tension-compression loading, the tension-tension loading rig was modified so that the plunger had a line contact with both the top and bottom surfaces of the beam, instead of line contact with just the top surface.

observed stress-life (*S/N*) behavior at $R = 0.1$ in human dentin, with apparent fatigue limits at 10^6-10^7 cycles of ~ 25 and 45 MPa at frequencies of 2 and 20 Hz, respectively. [The endurance strength is defined as the stress-amplitude to yield a specific life, generally 10^6 cycles or above. If the *S/N* curve is horizontal at this point, this is referred to as a fatigue limit, because below this stress-amplitude, the material, in principle, will never fail by fatigue.] Additionally, fatigue-crack growth rates (d*a*/d*N*), which we obtained by measuring specimen stiffness loss during cyclic loading, yielded a crack-growth law (in units of m/cycle, MPa$\sqrt{}$m) of:

$$da/dN = C\,(\Delta K)^m = 6.24 \times 10^{-11}\,(\Delta K)^{8.76} \qquad (1)$$

where ΔK is the stress-intensity range (difference in maximum and minimum stress intensities) and C and m are experimentally determined scaling constants. Taken as a whole, these studies represent only a limited understanding of how dentin responds to cyclic *vs.* mean stresses. To address this specific issue, the present work aims to document the role of the stress-ratio (*i.e.*, mean *vs.* alternating stress; Fig. 1a) in affecting the *in vitro* stress-life behavior of dentin over a wide range of stress-ratios from -1 (tension-compression loading) to 0.5 (tension-tension loading), and to analyze the resulting *S/N* curves (Fig. 1b) in terms of the classic Gerber (1874), Goodman (1899), and Söderberg (1939) approaches (Fig. 1c).

MATERIALS & METHODS

Materials

Human molars, recently extracted according to protocols approved by the University of California, San Francisco, Committee on Human Research, and by the Lawrence Livermore National Laboratory, were used in this study. We obtained samples by wet polishing (600-grit finish) sections (~ 1.5-2.0 mm thick) cut from the central portion of the crown and the root vertically through the tooth. Seventeen such beams (0.9-1.5 x 0.9-1.5 mm cross-section, 10.0-11.5 mm long) were used, with the long axes of the tubules aligned along the length of the beam. This "perpendicular" orientation (relative to the orientation of the crack plane) has the lowest toughness (*e.g.*, Rasmussen *et al.*, 1976; Nalla *et al.*, 2003b). In actuality, it is impossible to align the fracture plane precisely with the tubule axes *a priori* because, with the exception of the root, the tubules do not run a straight course from the enamel to the pulp. Rather, from the cervical margin through the crown, the tubules have a complex S-shaped curvature (Ten Cate, 1994). Hence, the precise orientation of the crack plane was determined afterward from examination of the fracture surfaces. *In vitro* first yield (σ_y) and maximum flexural tensile (σ_{ts}) strengths were measured in Hanks' Balanced Salt Solution (HBSS) in bending to be $\sigma_y \sim 75$ MPa and $\sigma_{ts} \sim 160$ MPa (Fig. 1d); these values were used for selection of stress levels for fatigue testing and in the constant-life approach. All specimens were kept hydrated throughout preparation and testing.

Stress-life (*S/N*) Fatigue Testing

In vitro S/N fatigue tests were conducted in HBSS at 37°C with unnotched cantilever beams (Fig. 1e) cycled on an ELF® 3200-

series machine (EnduraTEC Inc., Minnetonka, MN, USA). Testing was performed at three stress-ratios, R = -1, 0.1, and 0.5, at a constant frequency of 10 Hz. Beams were cycled to failure under displacement control, with loads continuously monitored. *S/N* curves were determined in terms of the stress-amplitude, σ_a, and the mean-stress, σ_m, based on the nominal bending-stress in the beam (Fig. 1a). The minimum and maximum stresses were chosen to give lives between 10^3 and 10^7 cycles; values ranged between, respectively, -96 and 96 MPa for R = -1, 6 and 155 MPa for R = 0.1, and 46 and 158 MPa for R = 0.5.

Fractography

Fracture surfaces were examined by scanning electron microscopy (SEM) (back-scattered mode). Surfaces were sputter-coated with a gold-palladium alloy prior to being imaged. To minimize the possibility of damage during preparation, we hydrated the beams until actual sputter-coating was performed.

RESULTS

Stress-life Fatigue Behavior

Stress-life (*S/N*) data are shown in Fig. 2a in the form of number of fatigue cycles to failure, N_f, as a function of the stress-amplitude, σ_a. Fatigue data spanning greater than three decades of lifetimes (~ 10^3 to > 10^6 cycles) are shown (each data point represents the reported lifetime from a single specimen). *S/N* data for various stress-ratios (R = -1, 0.1, and 0.5) at a constant frequency (10 Hz) and various frequencies (2, 10, and 20 Hz; 2 and 20 Hz data from Nalla *et al.*, 2003a) at constant stress-ratio (R = 0.1), are shown in Figs. 2a and 2b, respectively.

For R = -1, the stress-amplitude at zero mean-stress, σ_{ao}, can be mathematically related to the number of stress reversals, $2N_f$, to failure (twice the number of cycles) by the Basquin (1910) formulation:

$$\sigma_{ao} = \sigma_f (2N_f)^b \qquad (2)$$

where σ_f is the fatigue-strength coefficient and b is the fatigue-strength exponent (Morrow, 1968). Regression analysis gives values of σ_f = 247 MPa and b = -0.111 (coefficient of determination, R^2 = 0.9) for the relevant data in Fig. 2. However, Eq. 2 is valid only for the case of zero mean-stress (R = -1); to account for tensile mean-stresses, σ_m, on the fatigue lifetime, Morrow's (1968) modification of Eq. 2 can be used:

$$\sigma_{am} = (\sigma_f - \sigma_m)(2N_f)^b = (247 - \sigma_m)(2N_f)^{-0.111} \qquad (3).$$

This formulation yields more reasonable estimates for lifetimes at R = 0.1 (R^2 = 0.8), as compared with R = 0.5 (R^2 = 0.6). Overall, Eq. 3 can be utilized to reasonably predict the fatigue lifetime for any mean-stress/stress-amplitude combination.

Fractographic Observations

Scanning electron micrographs of the fatigue fracture surfaces show no major differences at different stress-amplitudes or tensile stress-ratios (Figs. 3a, 3b). However, for tension-compression cycling (R = -1), damage from crack-surface contact during the compressive portion of the cycle is evident as flat, featureless regions on the fracture surface (Fig. 3c). These regions were found on both sides of the fracture surfaces, and thus were not artifacts of specimen preparation.

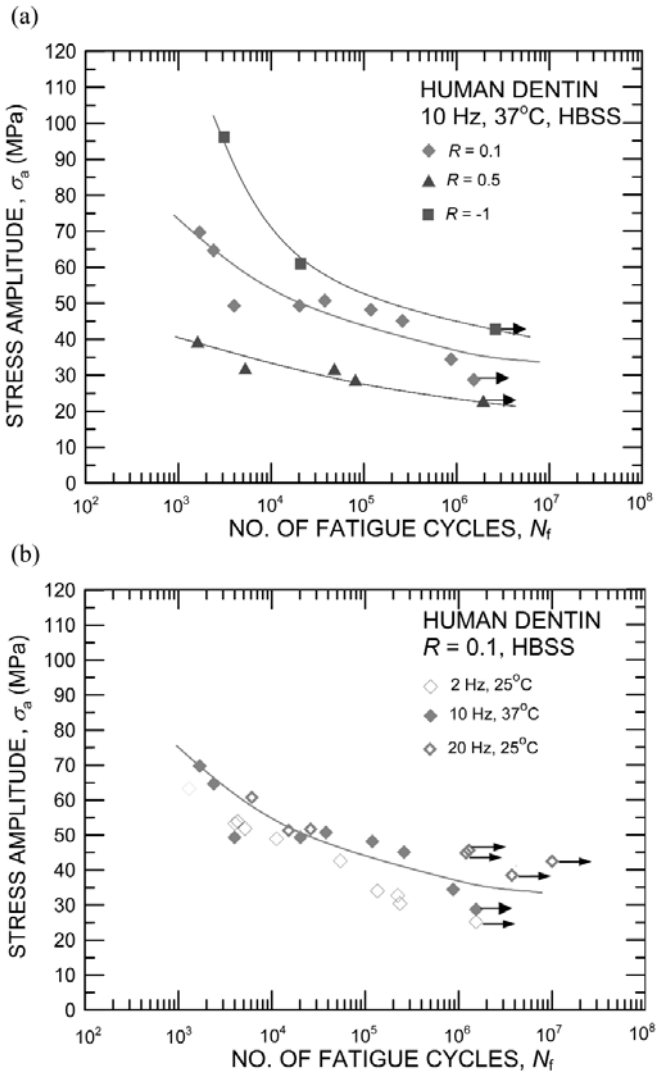

Figure 2. Stress-life (*S/N*) data obtained for human dentin in HBSS at 37°C in the form of the stress-amplitude, σ_a, as a function of the number of cycles to failure, N_f. Results are shown **(a)** for various stress-ratios at a constant frequency (10 Hz), and **(b)** for various frequencies at constant stress-ratio (R = 0.1). Horizontal arrows represent samples that did not fail ("run-outs").

DISCUSSION

In common engineering parlance, fatigue refers to the response of a material to repeated application of stress or strain. For most structural components, the prediction of number of cycles to failure under such repetitive loading is often a crucial step for design and durability assurance. The traditional *S/N* approach used herein serves to determine the cycles required to induce failure of *nominally* flaw-free samples loaded at specific alternating- and mean-stresses (as in Fig. 1b); the consequent fatigue lifetime therefore represents the cycles to both initiate and propagate a crack to failure.

Consistent with previous studies (Nalla *et al.*, 2003a), dentin

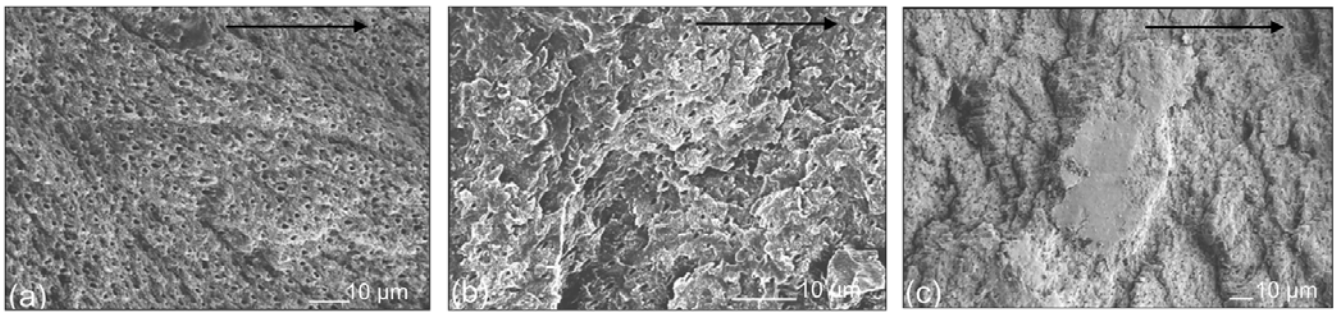

Figure 3. Scanning electron micrographs of the typical fracture surfaces for the three stress-ratios investigated. Note that there are no significant differences between the appearance of the fracture surfaces for the tensile stress-ratios, *R* of 0.1 and 0.5, as shown in **(a)** and **(b),** respectively. For the tension-compression stress-ratio, *R* of -1 in **(c),** damage from fracture surface contact is evident. The black arrow in each fractograph gives the direction of nominal crack growth.

was seen to display "metal-like" stress-life behavior, with an apparent fatigue limit for lives in excess of 10^6 cycles (Fig. 2a). The fatigue lifetimes (i) decrease with increasing stress-amplitudes (at a given stress-ratio), (ii) decrease with increasing tensile mean-stress (at a given stress-amplitude), (iii) decrease with increasing stress ratio (at a given stress-amplitude), and (iv) display an apparent plateau, resembling a fatigue limit, at lives greater than 10^6 cycles. In fact, the 10^6-cycle endurance strength is reached at a stress-amplitude of roughly 45 MPa, *i.e.*, ~ 0.3 of the measured tensile strength, for tension-compression loading. This is similar to that seen in most metallic alloys, where the fatigue limit or 10^6-cycle endurance strength (strictly defined at $R = -1$) is some 30-50% of the (single-cycle) tensile strength (Morrow, 1968). In dentin, the endurance strength is reduced with increasing stress-ratio to ~ 30 MPa (~ $0.2\sigma_{ts}$) for nominally zero-tension ($R = 0.1$) loading, and to just above 20 MPa (~ $0.15\sigma_{ts}$) at $R = 0.5$. The behavior at $R = 0.1$ is also consistent with that reported previously (Nalla *et al.*, 2003a) for testing in 25°C HBSS at 2 and 20 Hz. The two data sets are compared in Fig. 2b; while there is little effect of temperature over this narrow range, an effect of cyclic frequency is evident, particularly at longer lifetimes.

The effect of mean-stress on the fatigue lifetime is often represented in terms of constant-life diagrams (Fig. 1c) (Goodman, 1899). Here, the fatigue data are plotted as stress-amplitude/mean-stress combinations that result in similar fatigue lifetimes. Three empirical models, due to Gerber (1874), Goodman (1899), and Söderberg (1939), are commonly used:

$$\text{Gerber relation:} \quad \sigma_a = \sigma_{ao}\left[1 - \left(\frac{\sigma_m}{\sigma_{ts}}\right)^2\right] \qquad (4)$$

$$\text{Goodman relation:} \quad \sigma_a = \sigma_{ao}\left(1 - \frac{\sigma_m}{\sigma_{ts}}\right) \qquad (5)$$

$$\text{Söderberg relation:} \quad \sigma_a = \sigma_{ao}\left(1 - \frac{\sigma_m}{\sigma_y}\right) \qquad (6)$$

where σ_a and σ_m are, respectively, the stress-amplitude and mean-stress to give a specific lifetime for a finite mean-stress ($\sigma_m \neq 0$), σ_{ao} is the stress-amplitude to give the same life under fully reversed loading ($\sigma_m = 0$, $R = -1$), and σ_{ts} and σ_y are the tensile and yield strengths, respectively. Söderberg's approach is the most conservative; the Goodman line usually matches data for many brittle metallic alloys, and the Gerber parabola for more ductile materials (Morrow, 1968).

In Fig. 4, the stress-life data are plotted in the form of such constant-life diagrams. For ease of representation of lines of constant life, the data are redistributed into three groups: $N_f < 5 \times 10^3$, $5 \times 10^3 < N_f < 5 \times 10^5$, and $N_f > 5 \times 10^5$ cycles. It is apparent that the Gerber parabola gives the best representation of the fatigue results at lower lifetimes (~ 10^3-10^4 cycles) (Fig. 4a), whereas the Goodman line is more accurate at longer lifetimes (~ 10^6 cycles) (Fig. 4b). In fact, most of the data lie between the Goodman and Gerber lines. Consistent with behavior for many engineering alloys (Suresh, 1998), the Söderberg line was too conservative (Fig. 4c).

With the Gerber and Goodman lines, respectively, as upper and lower bounds (Fig. 4d), these diagrams can provide a reasonable definition of safe and unsafe regions for *in vitro* fatigue failure of dentin. For example, if the loading involves a maximum stress of 50 MPa and a minimum stress of -50 MPa (σ_a = 50 MPa, σ_m = 0 MPa), failure would probably occur in under one million cycles. Conversely, a maximum stress of 25 MPa and a minimum stress of -15 MPa (σ_a = 20 MPa, σ_m = 5 MPa) are unlikely to induce failure in a million cycles. Since human teeth experience ~ 5×10^5 to 10^6 loading cycles *per* year with typical masticatory stress levels on the order of 20 MPa (Anderson, 1956), the current results are comforting, since the *S/N* approach does not predict failures in dentin under these conditions (except perhaps with very high mean stresses), since stresses lie below the relevant endurance strengths.

In summary, *S/N* data are presented for *in vitro* fatigue of human dentin over a wide range of alternating stresses (involving tension and compression loading), tensile mean-stresses, and stress-ratios from -1 to 0.5. The results are quantified in terms of both (i) a mean-stress modified Basquin equation to describe the relationship between applied mean/alternating stresses and lifetime, and (ii) constant-life diagrams based on the Gerber, Goodman, and Söderberg relationships. It was found that human dentin displays "metal-like" *S/N* behavior with an apparent fatigue limit. To account for the effects of tensile mean-stresses, the lifetime data were found to be bounded by the Gerber parabola at lower lives and by the Goodman line at longer lives. By using these relationships, we

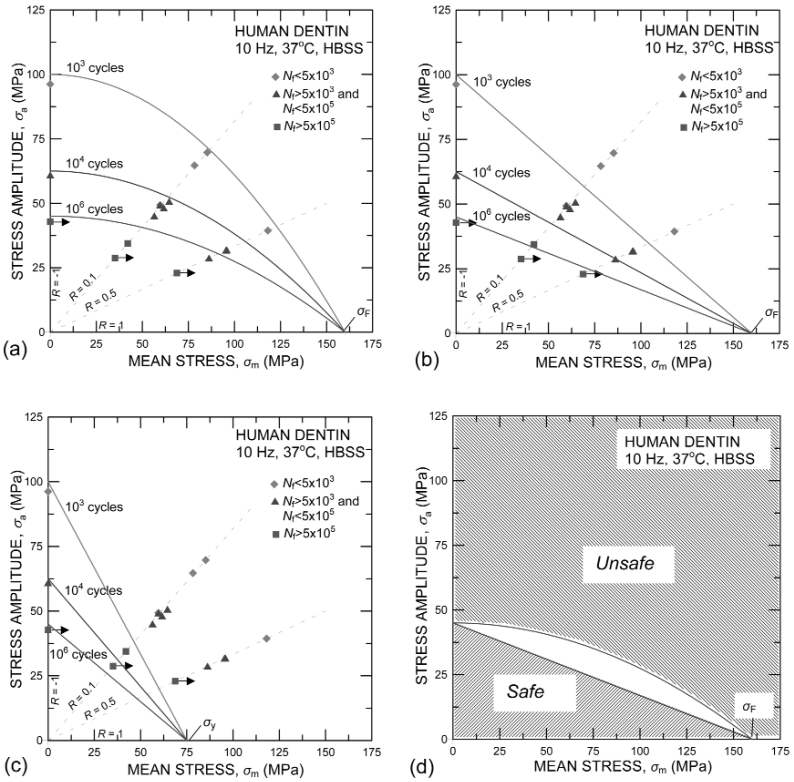

Figure 4. Fatigue data re-plotted as stress-amplitude *vs.* mean-stress, σ_a - σ_m combinations that result in similar fatigue lifetimes, N_f. Also shown are the **(a)** Gerber, **(b)** Goodman, and **(c)** Söderberg models. **(d)** The Goodman and Gerber models are shown encompassing the fatigue data; the safe and unsafe regions for 10^6-cycle lifetimes are also indicated.

have been able to span the entire range of possible load/unload conditions with relatively few *S/N* measurements. These results suggest that an undamaged tooth is designed not to fail from normal mastication. However, it should be noted that our measurements have been made with undamaged specimens in a controlled environment and a single orientation. Therefore, it is possible that these fatigue measurements may not provide a conservative estimate for tooth lifetimes. Further studies designed to include such potentially deleterious effects are warranted. Nevertheless, these results are of significance for the development of a micro-mechanistic understanding of how cyclic-fatigue loading can affect the behavior of human dentin, with consequent implications for lifetime prediction.

ACKNOWLEDGMENTS

This work was supported by Grant #P01DE09859 from National Institutes of Health/National Institute of Dental and Craniofacial Research and by Grant #DE-AC03-76SF00098 from the US Department of Energy, Office of Science-Basic Energy Sciences, Division of Materials Sciences and Engineering (for ROR). The authors thank Grace Nonomura for specimen preparation.

REFERENCES

Anderson DJ (1956). Measurement of stress in mastication I. *J Dent Res* 35:664-670.

Arola D, Rouland JA, Zhang D (2002). Fatigue and fracture of bovine dentin. *Exp Mech* 42:380-388.

Basquin OH (1910). The exponential law of endurance tests. *Proc Am Soc Test Mater* 10:625-630.

Craig RG, Peyton FA (1958). Elastic and mechanical properties of human dentin. *J Dent Res* 37:710-718.

Gerber H (1874). Bestimmung der Zulässigen Spannungen in Eisen-konstruktionen. *Z Bayer Arch Ingenieur-Vereins* 6:101-110.

Goodis HE, Marshall GW Jr, White JM, Gee L, Hornberger B, Marshall SJ (1993). Storage effects on dentin permeability and shear bond strengths. *Dent Mater* 9:79-84.

Goodman J (1899). Mechanics applied to engineering. London: Longmans Green.

Jones S, Boyde A (1984). Ultrastructure of dentin and dentinogenesis. In: Dentin and dentinogenesis. Linde A, editor. Boca Raton: CRC Press, pp. 81-134.

Kinney JH, Marshall SJ, Marshall GW (2003). The mechanical properties of human dentin: a critical review and re-evaluation of the dental literature. *Crit Rev Oral Biol Med* 14:13-29.

Lehman ML (1967). Tensile strength of human dentin. *J Dent Res* 46:197-201.

Levitch LC, Bader JD, Shugars DA, Heymann HO (1994). Non-carious cervical lesions. *J Dent Res* 22:195-207.

Morrow JD (1968). Fatigue design handbook. In: Advances in engineering. Vol. 4. Warrendale: Society of Automotive Engineers, pp. 21-29.

Nalla RK, Imbeni V, Kinney JH, Staninec M, Marshall SJ, Ritchie RO (2003a). *In vitro* fatigue behavior of human dentin with implications for life prediction. *J Biomed Mater Res* 66(A):10-20.

Nalla RK, Kinney JH, Ritchie RO (2003b). Effect of orientation on the in vitro fracture toughness of dentin: the role of toughening mechanisms. *Biomaterials* 24:3955-3968.

Rasmussen ST, Patchin RE, Scott DB, Heuer AH (1976). Fracture properties of human enamel and dentin. *J Dent Res* 55:154-164.

Sano H, Ciucchi B, Matthews WG, Pashley DH (1994). Tensile properties of mineralized and demineralized human and bovine dentin. *J Dent Res* 73:1205-1211.

Söderberg CR (1939). Factor of safety and working stress. *Trans Am Soc Mech Eng* 52:13-28.

Suresh S (1998). Fatigue of materials. 2nd ed. Cambridge: Cambridge University Press.

Ten Cate AR (1994). Oral histology. In: Development, structure and function. Vol. 4. St. Louis: Mosby, p. 173.

Tonami K, Takahashi H (1997). Effects of aging on tensile fatigue strength of bovine dentin. *Dent Mater J* 16:156-169.

Wiskott HW, Nicholls JJ, Belser UC (1995). Stress fatigue: basic principles and prosthodontic implications. *Int J Prosthodont* 8:105-116.